Received: 26 December 2017 | Accepted: 10 September 2018

DOI: 10.1111/1365-2745.13076

RESEARCH ARTICLE

Journal of Ecology | BRITISH ECOLOGICAL SOCIETY

Fire, fragmentation, and windstorms: A recipe for tropical forest degradation

Divino V. Silvério[1,2] | Paulo M. Brando[1,3] | Mercedes M. C. Bustamante[2] | Francis E. Putz[4] | Daniel Magnabosco Marra[5,6,7] | Shaun R. Levick[5,8] | Susan E. Trumbore[5]

[1]Instituto de Pesquisa Ambiental da Amazônia, Mato Grosso, Brasil; [2]Departamento de Ecologia, Universidade de Brasília, Brasília, Brazil; [3]The Woods Hole Research Center, Falmouth, Massachusetts; [4]Department of Biology, University of Florida, Gainesville, Florida; [5]Department of Biogeochemical Processes, Max Planck Institute for Biogeochemistry, Jena, Germany; [6]Laboratório de Manejo Florestal, Instituto Nacional de Pesquisas da Amazônia, Manaus, Brazil; [7]AG Spezielle Botanik und Funktionelle Biodiversität, Universität Leipzig, Leipzig, Germany and [8]CSIRO Land and Water, Winnellie, NT, Australia

Correspondence
Divino V. Silvério
Email: divino.silverio@ipam.org.br

Funding information
Brazilian National Council for Scientific and Technological Development (CNPq), Grant/Award Number: 150212/2015-11 , 307084/2013-2 and 405800/2013-4; Brazilian Agricultural Research Corporation (EMBRAPA); US Forest Service; USAID; Department of State

Handling Editor: David Edwards

Abstract

1. Widespread degradation of tropical forests is caused by a variety of disturbances that interact in ways that are not well understood.
2. To explore potential synergies between edge effects, fire and windstorm damage as causes of Amazonian forest degradation, we quantified vegetation responses to a 30-min, high-intensity windstorm that in 2012, swept through a large-scale fire experiment that borders an agricultural field. Our pre- and postwindstorm measurements include tree mortality rates and modes of death, above-ground biomass, and airborne LiDAR-based estimates of tree heights and canopy disturbance (i.e., number and size of gaps). The experimental area in the southeastern Amazonia includes three 50-ha plots established in 2004 that were unburned (*Control*), burned annually (*B1yr*), or burned at 3-year intervals (*B3yr*).
3. The windstorm caused greater damage to trees (>10 cm DBH) in the burned plots (*B1yr*: 13 ± 9% of 785 trees; *B3yr*: 17 ± 13% of 433) than in the *Control* plot (8 ± 4% of 2,300; ± CI). It substantially reduced vegetation height by 14% in *B1yr*, 20% in *B3yr* and 12% in the *Control* plots, while it reduced above-ground biomass by 18% of 77.7 Mg/ha (*B1yr*), 31% of 56.6 (*B3yr*), and 15% of 120 *(Control)*. Tree damage was greatest near the agricultural field edge in all three plots, especially among large trees and in *B3yr*. Trunk snapping (70%) and uprooting (20%) were the most common modes of tree damage and mortality, with the height of trunk failure on the burned plots often corresponding with the height of historical fire scars. Of the windstorm-damaged trees, 80% (*B1yr*), 90% (*B3yr*), and 57% (*Control*) were dead 4 years later. Trees that had crown damage experienced the least mortality (22%–60%), followed by those that were snapped (55%–94%) and uprooted (88%–94%).
4. *Synthesis*. We demonstrate the synergistic effects of three kinds of disturbances on a tropical forest. Our results show that the effects of windstorms are exacerbated by prior degradation by fire and fragmentation. We highlight that understorey fires can produce long-lasting effects on tropical forests not only by directly

killing trees but also by increasing tree vulnerability to wind damage due to fire scars and a more open canopy.

KEYWORDS
Amazonia, biomass loss, fire scar, forest degradation, forest dynamics, tree mortality, windstorms

1 | INTRODUCTION

Disturbances shape the structure and affect the dynamics of tropical forests (Attiwill, 1994; Brando et al., 2014; Negrón-Juárez et al., 2010; Trumbore, Brando, & Hartmann, 2015). By killing and damaging trees, they alter forest carbon stocks and fluxes (Espírito-Santo et al., 2014; Vanderwel, Coomes, & Purves, 2013), diversity and composition (Marra et al., 2014), and the spatio-temporal variability of forest dynamics (Chambers et al., 2013; Vanderwel et al., 2013). In the Amazonia Basin alone, wind disturbances are estimated to cause temporary reductions in above-ground forest biomass of ~1.7 Pg/year (Espírito-Santo et al., 2014). While forests in this region have experienced droughts, fires, and windstorms for millennia (Cole, Bhagwat, & Willis, 2014; Ledru, 2001; Mayle et al., 2008), disturbance regimes are now changing in response to climate and land-use change (Duffy, Brando, Asner, & Field, 2015; Emanuel, 2013; McDowell et al., 2018). There is growing evidence that a strong shift in disturbance frequency, intensity, and extent could push the Amazonia region into an alternate state (Brando et al., 2014; Emanuel, 2013; McDowell et al., 2018), potentially releasing to the atmosphere a large part of the ~120 Pg of above-ground forest biomass that remain in the pan-Amazonia intact forests (Mitchard et al., 2014).

Windstorms are among the most common natural forest disturbances in Amazonia (Chambers et al., 2013; Espírito-Santo et al., 2014; Marra et al., 2014; Negrón-Juárez et al., 2010; Rifai et al., 2016). Downbursts associated with convective systems that produce strong vertical descending wind gusts are particularly noteworthy because their effects range from the breakage of individual branches or single treefalls to blowdowns of thousands of hectares (Garstang, White, Shugart, & Halverson, 1998; Nelson, Kapos, Adams, Oliveira, & Braun, 1994). For example, a squall line that moved from SW to NE Amazonia in 2005 damaged extensive forested areas (Negrón-Juárez et al., 2010) especially in central Amazonia, although the number of damaged trees remains uncertain (Araujo, Nelson, Celes, & Chambers, 2017). Wind impacts on closed forest canopies are known to vary with storm strength (Canham, Thompson, Zimmerman, & Uriarte, 2010), topography (de Toledo, Magnusson, Castilho, & Nascimento, 2012; Rifai et al., 2016), and tree structural characteristics such as wood density (Putz, Coley, Lu, Montalvo, & Aiello, 1983; Rifai et al., 2016), whole-tree flexibility (Asner & Goldstein, 1997), height–diameter ratio (Hurst, Allen, Coomes, & Duncan, 2011), and size (Rifai et al., 2016). Depending on how these variables interact during a windstorm event, tropical trees can have their crowns damaged, trunks snapped, or roots pulled from the ground (uprooted).

Deforestation could amplify the effects of windstorms on Amazonian forests via several mechanisms. Firstly, forest clearing for pasture and cropping changes local convective circulation patterns and results in strong advective winds near forest edges (Bull & Reynolds, 1968; Durieux, Machado, & Laurent, 2003; Jiao-jun, Xiu-fen, Yutaka, & Takeshi, 2004; Mahmood et al., 2014; Weaver & Avissar, 2001), increasing overall wind stresses on trees near edges (Bull & Reynolds, 1968). Secondly, large trees exposed along recently created forest edges have few adaptations to resist strong winds (Holbrook & Putz, 1989). Thus, windstorms are expected to be most damaging to trees growing along edges of recently cleared fields (Laurance & Curran, 2008). In southeastern Amazonia, forest edges (i.e., <200 m from an open agricultural field) now account for ~12% of the remaining forests (Brando et al., 2014). As deforestation increases the fragmentation of intact forests over increasingly large areas (Hansen et al., 2013; INPE, 2016), wind-related disturbances can be expected to increase. For example, Schwartz et al. (2017) showed that forest degradation by fragmentation and windstorms has already degraded large tracts of forests.

Fires modify forest structure and filter some traits that may change residual tree vulnerability to wind damage. For example, fires tend to kill trees with low wood density and thin bark (Brando et al., 2012), thereby filtering out trees that are more susceptible to wind damage. On the other hand, forest fires may amplify the effects of windstorms on tropical forests by damaging trunks and thus compromising tree stability. Such a process could help explain the delayed postfire mortality of large trees observed in various tropical forests (Baker, Bunyavejchewin, & Robinson, 2008; Barlow, Peres, Lagan, & Haugaasen, 2003). Apart from damaging tree trunks, forest fires are expected to increase wind-related damage by decreasing canopy cover (Balch et al., 2008) and thereby increasing the torque that wind exerts on individual crowns (Garstang et al., 1998). Furthermore, reductions in tree density leading to changes in root systems and consequently in tree-anchoring capacity (Hurst et al., 2011) may increase residual tree proneness to uprooting.

Forest fragmentation, fires, and windstorms each cause some level of forest disturbance in Amazonia (Brando et al., 2014; Broadbent et al., 2008; Chambers et al., 2013; Haddad et al., 2015; Negrón-Juárez et al., 2010), but if they act synergistically, the impacts on forest structure, dynamics, and carbon stocks could be amplified. Most of the current understanding on the effects of wind disturbances on Amazonia forests derives from studies that quantified the

spatial extent of blowdown events using remote sensing imagery (Chambers et al., 2013; Espírito-Santo et al., 2014; Negrón-Juárez et al., 2010) or from postdisturbance field inventories, which often lag the windstorm event by many months or years (Marra et al., 2014; Schwartz et al., 2017). While these studies have shown that wind disturbance exerts strong influences on the structure and diversity of tropical forests, they often lack mechanistic approaches to understand how forests respond to synergistic interactions between windstorms and other forest disturbances.

In this study, we address the knowledge gap of how the combined effects of fragmentation, fire, and windstorms affect tree mortality and above-ground biomass in a southeastern Amazonian forest. Our study area was subjected to experimental surface fires from 2004 to 2010 during the dry-season peak. The initial experimental fires caused lower-than-expected alterations in forest structure and diversity (Balch et al., 2008), with leaf area index (LAI) decreasing by only 20% and mortality rates increasing by only 3% compared with an unburned Control. However, recurrent fires that coincided with the droughts of 2007 and 2010 killed a high proportion of trees. For instance, we observed the mortality of 33%–84% of trees with diameter at breast height >10 cm growing near the neighbouring agricultural field. We also observed more fire-induced tree mortality in the plot burned every 3 years (*B3yr*) than in the one burned every year (*B1yr*) (Brando et al., 2014). In response to the more intense fires in drought years, above-ground biomass in the burned plots was reduced to 49%–55% of the *Control* plot, creating opportunities for grasses to invade along much of the forest edge (Brando et al., 2014, 2012; Silverio et al., 2013). In general, fire effects were most severe for small trees as well as for those with low wood density and thin bark (Brando et al., 2012). Thus, postfire communities contained more large trees with high wood density and thick bark.

Our plots, which border an agricultural field, were inventoried 1 month before and 1–4 days after a major windstorm event—a unique opportunity to evaluate the effects of wind on tropical forest structure. We hypothesized that tree vulnerability to wind damage is higher along forest edges than in forest interiors. We also hypothesized that more trees in the burned plots would be susceptible to wind damage due to fire scars and modified forest structure even though burned forests have more trees with high wood density that should render them more resistant to wind damage. We also predicted that the likelihood of wind damage was higher among larger and more exposed trees, which tend to experience stronger wind-related torque.

2 | MATERIALS AND METHODS

2.1 | Study area and experimental design

This study was conducted in a forest located in the southern portion of the Amazonia Basin (13°04′ S, 52°23′ W; Figure 1). We quantified the effects of a windstorm that occurred on October 25, 2012 and affected an experimental forest that borders an agricultural field with three 50-ha permanent plots: one unburned (*Control*), one burned every year (*B1yr*), and one burned every 3 years (*B3yr*) between 2004 and 2010 (Figure 1a; see details in Balch et al., 2008). The agricultural field facing the experimental plots was used as pasture for over 20 years until 2007, when it was converted into a soybean field.

Annual precipitation in our study area averages 1,700 mm and is concentrated during the October–April wet season. The annual temperature averages 25°C with 71% relative humidity. The studied windstorm occurred on October 25, 2012, lasted for 30 min, and was witnessed by DS and PB. During the half hour in which the event lasted, the average air temperature and relative humidity recorded at a weather station 1 km from the experimental plots averaged 27.5 ± 1.3°C and 94.9 ± 6.1% respectively (±CI). The average wind speed was 52 km/h (maximum speed was not recorded) and wind direction was from 16 ± 15° (±CI) (Figure 1b). Based on the Beaufort scale, which is an empirical measure of wind speed according to observed effects of wind on land, including snapped and uprooted trees (Huler, 2004) we estimated the maximum wind speeds to be above 90 km/h. At the site, total precipitation on the day of the storm was 76 mm. Daily precipitation across the region was 83 mm (as estimated from the Tropical Rainfall Measuring Mission; Supporting Information Figure S1), which suggests that the studied storm was not restricted to our field site.

2.2 | Airborne LiDAR surveys to quantify forest structural changes

We used two airborne LiDAR surveys, one from before (April 2012) and another 2 years after the studied windstorm (October 2014). Airborne LiDAR data were collected by the GEOID Ltda Company as part of the Sustainable Landscapes Brazil, a joint project of the Brazilian Corporation of Agricultural Research (EMBRAPA) and the United States Forest Service (USFS). The study area was flown at an average altitude of 850 m a.s.l. and a total area of approximately 1,005 ha was covered. An Optech ALTM-3100 laser scanner was used in 2012 and an Optech ORION-09SEN243 in 2014; average return densities were 13.7/m^2 in 2012 and 41.05/m^2 in 2014. The original LiDAR dataset and associated metadata are freely available on https://mapas.cnpm.embrapa.br/paisagenssustentaveis/. Full- and reduced-density datasets were processed to generate the Canopy Height Model (CHM) above-ground raster layers at 1-m resolution. CHM products were generated using the G-LiHT algorithm (Cook et al., 2013) by selecting the highest LiDAR return in every 1-m grid cell, building a triangulated irregular network (TIN) based on these points, and interpolating canopy heights on a 1-m raster grid.

2.3 | Quantification of individual tree damage and mortality

Our quantification of wind-related impacts on forest structure and tree mortality was based on three forest transect inventories: (a) a prewindstorm inventory (conducted between 1 August and 15 September, 2012) in which all trees on six transects crossing

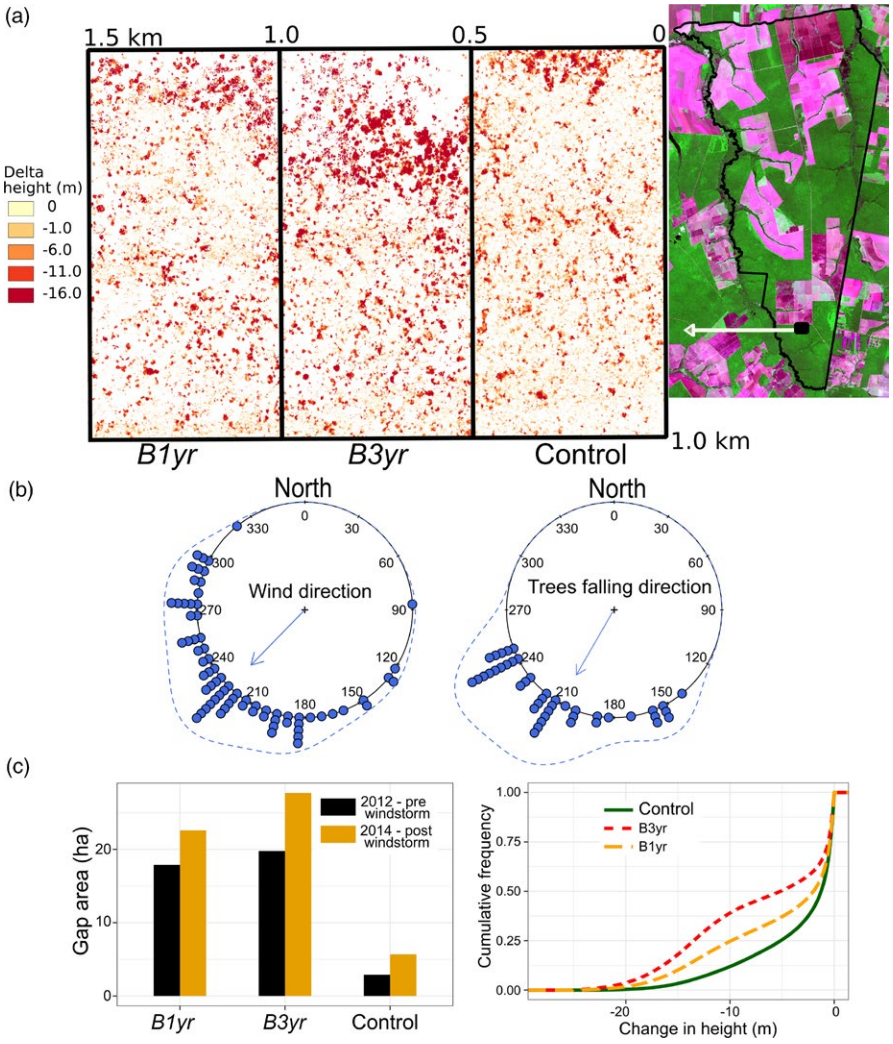

FIGURE 1 The experimental area in southwestern Amazonia where we evaluated the impacts of a 2012 windstorm. Between 2004 and 2010, the three 50-ha plots were burned either annually (*B1yr*), burned triannually (*B3yr*), or not burned at all (*Control*). The upper panel (a) highlights the spatial patterns of change in forest height (as estimated by airbone LiDAR) between 2012 and 2014 (before and after the windstorm respectively) (left), and a Landsat RGB image that shows the location of the experimental area on the landscape (right). Dark green indicates forests and pink, the open agricultural field. The centre panel (b) shows the wind direction relative to magnetic north during the storm (left) and the directions trees in the *Control* plot fell when they were uprooted during the storm (right). The bottom panel (c) shows the area of gaps before and after the windstorm (left) and the cumulative frequency distribution of changes in forest height (right) [Colour figure can be viewed at wileyonlinelibrary.com]

the three fire treatment plots were recorded (detailed below); (b) a postwindstorm inventory of tree damage on the same transects conducted 1 hr after the windstorm; and (c) a postwindstorm inventory conducted 4 years after the windstorm (2016) to evaluate tree survival. In the pre- and poststorm inventories, we recorded all trees ≥10 cm DBH (diameter at breast height, 1.3 m) along six 1,500-m-long transects, 4 m and 18 m wide for trees 10–20 cm DBH and >20 cm DBH respectively. The transects ran parallel with the edge of the agricultural field at 10, 30, 100, 250, 500, and 750 m in from the edge. In each experimental plot we sampled 1.2 ha and 5.5 ha for trees 10–20 cm DBH and >20 cm DBH respectively (Figure 1). During the second forest inventory conducted shortly after the windstorm, we recorded damaged trees as: (a) *snapped*, when the trunk was broken above-ground but below the crown; (b) *uprooted*, when trees were completely toppled leaving roots exposed; and, (c) *crown damaged*, when trees lost more than 50% but less than their entire crown (Chambers, 2001; Marra et al., 2014; Ribeiro et al., 2016). We also recorded whether trees were directly affected by the windstorm or damaged by the fall of other trees. Four years after the windstorm (2016) we recorded whether trees assigned as *damaged* in our second inventory were dead or had resprouted. For each tree recorded in the first forest inventory we assigned a wood density value (Chave et al., 2006; Nogueira, Fearnside, Nelson, & França, 2007), measured the distance from the agricultural field edge, and quantified the number of live trees within a 20 m radius (estimated based on the LiDAR-derived canopy height model as detailed next). For species for which wood density data were not available (28%), we employed the mean wood density of congeneric species occurring in our study region.

We estimated the number of neighbours for each of the recorded trees with the 2012 LiDAR-derived CHM by using crown coordinates around each focal individual. We used a local maxima crown detection model (R package *rLIDAR*) that detects and computes the location and height of individual trees within the LiDAR-derived CHM above a specified height threshold. By using the location of each detected crown, we calculated the number of neighbours for all recorded trees within a radius of 20 m. A key input of the model is the minimum height threshold to stop detecting tree crowns, which was determined from inventory data as 11 m in the *Control* plot and 11.5 and 9.8 m for *B3yr* and *B1yr* respectively. This minimum height

threshold was the intercept of a linear regression between tree height (estimated using the LiDAR measurements) and DBH for each plot (i.e., the intercept for a 10 cm DBH tree).

2.4 | Statistical analyses

We tested our hypotheses with GLMs with binomial distributions and considered each type of damage in a different model. With this approach, we used the presence of damage on individual trees as a response variable to assess how the probability of wind damage varied with fire treatment (i.e., *Control*, *B1yr*, and *B3yr*), distance from the forest edge, tree size, wood density, and the number of neighbours within 20 m of a focal tree. We fit a global model using R (R Core Team, 2016) and assessed the importance of each predictor through a model selection procedure. We selected the most parsimonious models based on the Akaike information criterion (AIC) value (i.e., the lower the better, Supporting Information Tables S1 and S2; Zuur, Ieno, Walker, Saveliev, & Smith, 2009). Numeric predictors from the final models were not colinear (all $r < 0.52$; Supporting Information Table S3).

We tested for spatial autocorrelation (SA) in the model residuals using the Moran's I test and, when significant, we included the Moran eigenvector filters to remove SA from model residuals (Dray, Legendre, & Peres-Neto, 2006). The Moran's I test, as implemented by the *moran.test* function on the R-package *spdep* (Bivant, Altman, Anselin, Assunção, & Berke, 2016), uses matrix of spatial weights to test if a variable is clustered, dispersed, or randomly distributed. Moran's I values range from +1.0 to −1.0, with values closer to +1 indicating clustering, and those closer to −1.0 indicating dispersion (Cliff & Ord, 1981). To correct for SA, when found, we used the Moran eigenvector filtering (Dray et al., 2006; Griffith & Peres-Neto, 2006), calculated by the *ME* function in the R-package *spdep* (Bivant et al., 2016). This procedure calculates eigenvectors that, when added to the GLM, reduce residual autocorrelation below the specified alpha value (Bivant et al., 2016; Griffith & Peres-Neto, 2006). We selected those eigenvectors that reduced residual autocorrelation below alpha = 0.05, and included these vectors as covariables in the best models, to remove SA.

To estimate the above-ground biomass before and after the windstorm, we employed a tree biomass estimation model that uses tree height, wood density, and DBH as predictors (Chave et al., 2005). The individual tree biomass predicted from the model were summed to yield stand values. We compared relative snapping heights between intact and fire-scarred trees with a Student's *t* test, and between the experimental plots (*Control*, *B1yr* and *B3yr*) with one-way analysis of variance (Zar, 1999). Throughout the text, we report means of measured attributes followed by confidence interval (±CI).

We used the pre- and poststorm LiDAR datasets to scale up our results from the transects to the entire experimental area. We used the CHMs derived from 2012 and 2014 campaigns to evaluate changes in canopy height, density, and size of canopy gaps. To calculate changes in canopy height, we subtracted the 2012 CHM from the 2014 CHM. We then evaluated the cumulative frequencies in height and the areas (Figure 1b) that experienced >5 m canopy height reductions. We used two approaches to estimate the number and size of gaps in the fire experiment. In both approaches, we applied the *PatchStat* function (R package *SDMTools*) that calculates patch statistics (VanDerWal, Falconi, Januchowski, & Storlie, 2015). In the first approach we used the 2012 and 2014 CHMs separately, which allowed us to quantify possible increases in the gap fraction. We considered gaps >5 m^2, with gap defined as an area where the canopy height was ≤10 m (see, Hunter et al., 2015). In the second approach, we applied the same gap-size threshold but only considered height reductions >10 m. We also used this second approach to evaluate changes in the number and area of gaps according to the edge distance for the three experimental plots and across all LiDAR transects bordering the agricultural field (Supporting Information Figure S7).

3 | RESULTS

3.1 | More snapping than uprooting

The windstorm affected 11% of the trees, of which 70% were snapped, 20% were uprooted, and 10% suffered major crown loss (Figure 2a). Of the damaged trees, 75% were directly damaged by the wind and 20% were struck by other trees (i.e., indirectly damaged). The predominant orientation of fallen trees (212 ± 33° to the magnetic north) aligns well with direction from which wind blew during the storm (196 ± 15°; Figure 1b). Among the 19 most common genera in our study area, *Tapirira* (Anacardiaceae), with individuals uniformly distributed across the plot (Supporting Information Figure S5), suffered the highest mortality rate and most damage (Figure 2b; 25% of the individuals snapped, uprooted, or crown damaged). In contrast, *Protium* (Burseraceae) and *Chaetocarpus* (Peraceae) were the least affected, with <5% of the individuals damaged (Figure 2b).

3.2 | More tree damage in previously burned areas

Although the storm damaged more trees in the unburned *Control* (184 trees) than in the burned plots (102 trees in *B1yr* and 78 trees in *B3yr*; Figure 2a), proportionally more trees were damaged in experimentally burned areas (*B1yr*: 12.7 ± 9.1%; *B3yr*: 17.4 ± 13.2%) than in the *Control* (8.3 ± 4.5%). For example, tree snapping in *B1yr* and *B3yr* averaged at 9.5% and 10.4%, respectively, whereas in the *Control* it averaged at only 5.6%. Also, more trees were uprooted in *B3yr* (6%) than in the other two treatment plots (*B1yr*: 1.9%; *Control*: 1.7%). Crown damage did not differ among the plots (Figure 2a).

Our results indicate that the presence of fire scars on tree trunks influenced the susceptibility of trees to snapping. More of the snapped trees in the burned plots had fire scars (*B3yr* = 70%; *B1yr* = 69%) than the uprooted ones (*B3yr* = 45%; *B1yr* = 25%). Also, the heights at which trees snapped were ~3 m lower in the burned plots (*B3yr* = 3.4 ± 0.6 m; *B1yr* = 3.3 ± 0.5 m) than in the *Control* (6.0 ± 0.5 m), which reflects the heights of fire scars. On average, unscarred trees snapped near the middle of the trees' trunks (46% of total tree height; *N* = 148) but

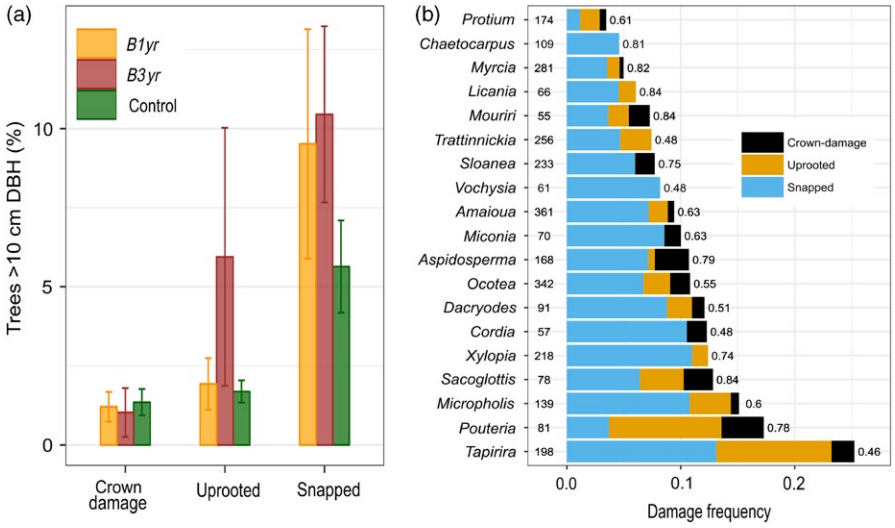

FIGURE 2 Percentage of individuals damaged during the 30-min windstorm on October 25, 2012 in southeastern Amazonia by type of damage in the three different fire treatments (*Control*, annual burns—*B1yr*, triennial burns—*B3yr*; standard error bars were calculated based on the six transects) (a), and proportion of damaged individuals of the 19 most abundant genera, number of recorded trees (on the left of bars) and mean wood density by genus (on the right of bars; g/cm^3) (b) [Colour figure can be viewed at wileyonlinelibrary.com]

fire-scarred trees snapped 25% lower (21% of the total height; $N = 83$; $t_{(117.1)} = 2.97$; $p = 0.003$). These results suggest that fire-damaged trees were more vulnerable to wind damage. The estimates of the GLM reinforce this notion; the presence of fire scars increased the probability of tree failure through snapping at any distance from the edge (Figure 3). Fire-scarred trees near the forest edge in *B3yr* or *B1yr* plots were 27%–34% more likely to be snapped than those without fire scars. Even fire-scarred trees >300 m from the edge were 9%–13% more likely to be snapped than those without fire scars (Figure 3). Although this pattern could be explained by a greater number of trees with fire scars growing along the forest edge than in the forest interior, the GLM showed that the interaction between fire scar and edge distance does not contribute to the solution fit (Supporting Information Table S1). Moreover, higher damage on the edge was consistent even for the *Control* plot that had no fire-scarred trees (Figure 3). The proportions of fire-scarred trees damaged by the storm along the forest edge (0–200 m) averaged at 69%, versus 56% in the forest interior (>200 m).

Our final GLM models showed a weak spatial dependence on the residuals (Supporting Information Figure S8) and the Moran's I test was not significant for Canopy ($I = -0.006$; $p = 0.74$), but it was for Snapped ($I = 0.09$; $p < 0.01$) and Uprooted damage ($I = 0.06$; $p < 0.01$). Fourteen Moran eigenvector filters were selected for the Snapped and two for the Uprooted damage and were included as covariables in the best models to remove the spatial autocorrelation (Supporting Information Table S2). The residuals of final model including the filters were not correlated with space for Uprooted ($I = 0.013$; $p = 0.08$) or Snapped ($I = 0.011$; $p = 0.1$).

Four years after the windstorm, 71% of the trees that were physically damaged were dead and only 29% had resprouted. We observed differences in mortality among treatments, with a lower proportional mortality among wind-damaged trees in the *Control* plot (57%) than in the *B1yr* and *B3yr* (80% and 90% respectively). Crown damaged trees experienced the least mortality (*Control* = 22%; *B3yr* = 40%; *B1yr* = 60%), followed by those that were snapped (*Control* = 55%; *B3yr* = 94%; *B1yr* = 80%) or uprooted (*Control* = 88%; *B3yr* = 93%; *B1yr* = 94%).

3.3 | Higher vulnerability to wind damage of large and edge-exposed trees

The likelihood of a tree suffering wind damage increased substantially with DBH for all treatments and types of damage (Figure 4). The probability of tree snapping and uprooting also increased with proximity to the agricultural field (Figure 3). For uprooted trees, this relationship was stronger in *B3yr* (primarily) and *B1yr* (secondarily) than in the *Control* (Figure 3d). Thus, a tree located in *B3yr* and close to the edge of the agricultural field was more likely to be uprooted than a tree located anywhere in *B1yr* or in the *Control* (Figure 3d). In addition to the observed higher damage in the burned plots (particularly in *B3yr*) and among large trees (especially those close to the forest edge), our statistical models showed that trees with lower wood density and with less neighbours were also more likely to be damaged by the windstorm (Supporting Information Tables S1 and S2; Supporting Information Figure S2). The probability of a tree being uprooted or snapped decreased as a function of increasing wood density (Supporting Information Figure S3).

3.4 | Changes in vegetation height and above-ground biomass

The windstorm caused an immediate 15% decline of above-ground live standing biomass in the *Control*, with declines of 18% in *B1yr*, and 31% in *B3yr* (Table 1). In addition, our LiDAR-based estimates of gap formation between 2012 and 2014, showed that 3,500 new gaps >5 m^2 were formed in the three 50-ha plots. More new gaps opened during the 2012–2014 period in the burned plots (*B3yr* = 37% [$n = 1{,}305$], *B1yr* = 34% [$n = 1{,}202$]) than in the *Control* (28% [$n = 994$]). Even though a large fraction of these new gaps (44%) was smaller than 15 m^2 (Supporting Information Figure S6), the total gap area in the 50 ha plots increased by 8.3 ha in *B3yr* (from 19.8 to 27.9 ha), 4.7 ha in *B1yr* (from 17.9 to 22.6 ha), and 2.8 ha in the *Control* (from 2.9 to 5.7 ha). Considering all LiDAR transects, gap formation between 2012 and 2014 was concentrated on the east of the transect, which coincides with our fire plots and the open field (Supporting

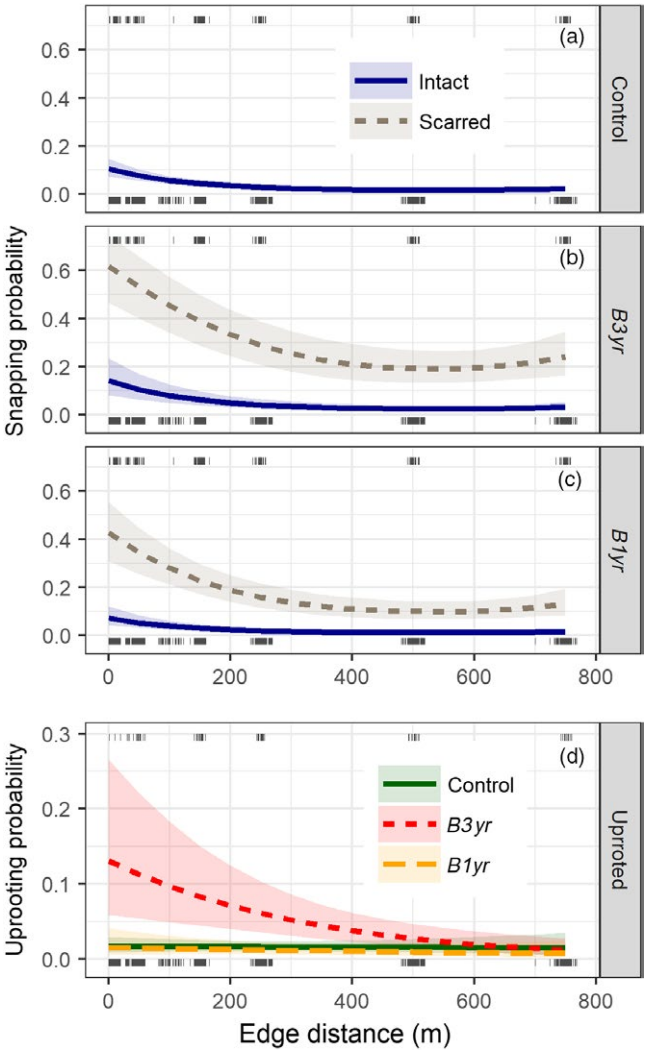

FIGURE 3 Probability of a tree being snapped as a function of distance from the forest edge and the presence of fire scars for the plot that was unburned (*Control*) (a), burned triennially (b), and annually (c), and the probability of a tree being uprooted for the three plots (d) as a function of distance from the forest edge based on logistic models. Shaded areas indicate 95% confidence intervals. Locations of damaged trees shown as small vertical lines above each graph with similar marks for undamaged trees below [Colour figure can be viewed at wileyonlinelibrary.com]

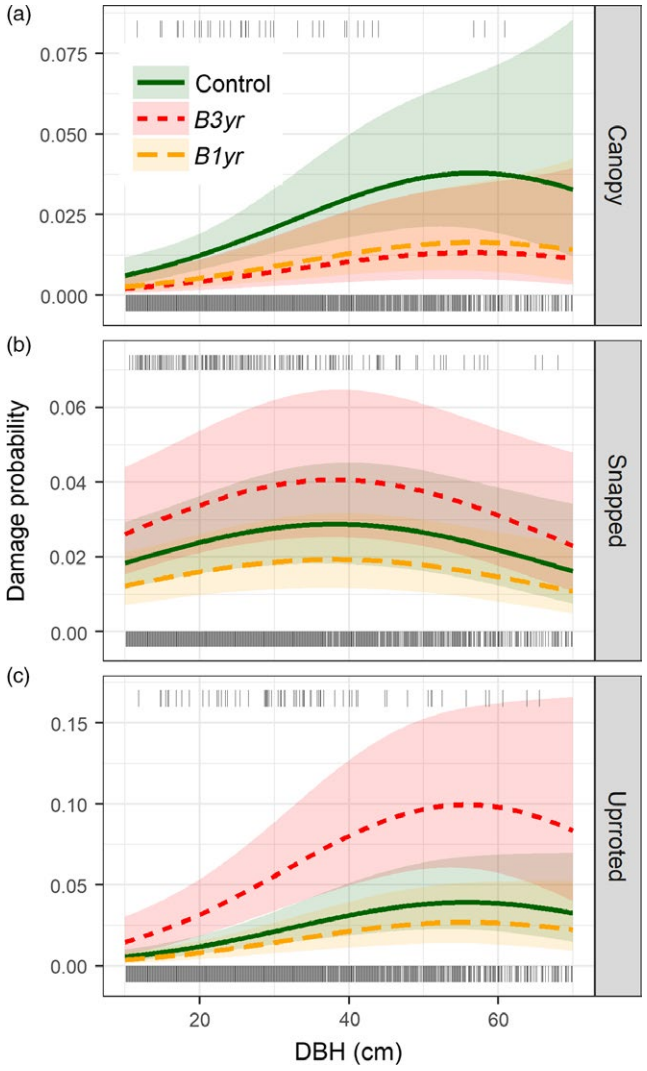

FIGURE 4 Wind damage probabilities as a function of DBH for the three plots (*Control*, annual burns—*B1yr*, triennial burns—*B3yr*) and for three types of damage: crown damage (a), snapped (b), and uprooted (c). Shaded areas indicate 95% confidence intervals. DBH (diameter at breast height) distribution of damaged trees are shown as small vertical lines above each graph with similar marks for undamaged trees below [Colour figure can be viewed at wileyonlinelibrary.com]

Information Figure S7). If only the nonburned forested portion of the LiDAR transect along the agricultural field is considered (265 ha), new gaps were also concentrated near the edge (Supporting Information Figure S7).

Our data suggest that most of the new gaps created between 2012 and 2014 were associated with the windstorm of 2012. The number and area of new gaps formed along our sampling transects (as estimated from LiDAR measurements) were positively correlated with the number of trees damaged by the windstorm (Supporting Information Figure S4). However, because the second LiDAR survey was conducted 2 years after the windstorm, it is possible that the high number of gaps estimated with LiDAR overestimates the effects of the windstorm alone. For example, annual tree mortality in the *Control* plot between 2005 and 2010 averaged at 4% (Table 1). Thus, considering the windstorm damage in the *Control* plot (8.3% of trees) and that normal tree mortality between 2012 and 2014 was similar to the observed in previous years (4%), we can assume that at least 50% of the observed increases in gap number and area captured by the LiDAR dataset were caused by the windstorm.

4 | DISCUSSION

We tested the overall hypothesis that forest fragmentation, fires, and windstorms interact synergistically to cause forest degradation. The 30-min windstorm we studied caused more tree damage and

TABLE 1 General information about the vegetation before the windstorm, breakage heights for snapped trees, and changes in above-ground biomass of trees >10 cm DBH (diameter at breast height) before and after a windstorm in two burned (*B3yr* and *B1yr*) plots and in a *Control* plot (50 ha each). Values are followed by confidence interval (±CI)

	Control	*B3yr*	*B1yr*
Vegetation characteristics			
Tree density before the windstorm (#/ha)	768	158	259
DBH median (cm)	16.6 ± 0.35	24.3 ± 0.91	21.9 ± 0.62
Wood density mean (g/cm^3)	0.63 ± 0.01^a	0.66 ± 0.01^b	0.67 ± 0.01^b
Tree mortality rate 2005–2010 (%/year)	4.0 ± 6.77	11 ± 6.33	9.4 ± 2.35
Above-ground biomass changes related to the windstorm			
Before (Mg/ha)	120.0 ± 6.05	56.6 ± 3.34	77.6 ± 4.06
After (Mg/ha)	102.4 ± 6.46	39.1 ± 4.42	63.9 ± 5.19
Change (%)	14.9	30.8	17.6
Total and breakage height for snapped trees			
Observed height of breakage (m)	5.96 ± 0.45^a	3.42 ± 0.66^b	3.40 ± 0.5^b
Total tree height (m)	16.21 ± 0.55^a	17.9 ± 0.96^a	16.3 ± 0.99^a
Height of breakage/total tree height	0.57 ± 0.09^a	0.19 ± 0.03^b	0.24 ± 0.03^b

Note. Means in the same line followed by the same letter do not differ at the 5% probability level by Tukey's tests.

death close to the forest edge, among large trees, and in previously burned areas. These results suggest that ongoing fragmentation and edge formation in tropical forests (Haddad et al., 2015; Hansen et al., 2013) can drive widespread forest degradation through increased vulnerability of standing trees to windstorms. Given that windstorm-related damage was highest in previously burned areas and for fire-scarred trees, forest degradation might also be intensified by changes in the climate through droughts that promote high-intensity fires (Brando et al., 2014; Duffy et al., 2015). These synergies and interacting processes are still not represented in many models used to predict the future structure and composition of tropical forests (Fisher et al., 2010; Nepstad, Stickler, Soares-filho, Merry, & Nin, 2008; Powell et al., 2013). Our results show that the inclusion of tree susceptibility to wind damage in such models could improve our understanding about the dynamics of old-growth and secondary Amazonia forests.

4.1 | Wind disturbance partially explains delayed tree mortality after fires

The effects of understorey fires on tropical forests may persist for several years due to delayed postfire tree mortality (Baker et al., 2008; Barlow et al., 2003). Our results suggest that windstorms could punctuate this pattern of delayed mortality by increasing tree mortality rates in previously burned areas. Two fire-related processes could explain this pattern: first, fire-damaged tree trunks are structurally weaker and, consequently, more vulnerable to wind breakage; second, by thinning the forest canopy (Balch et al., 2008; Brando et al., 2014), the fires increase the exposure of tree crowns to wind. Together, weakened tree trunks and more exposed crowns could cause higher rates of breakage in burned forests. By killing a large proportion of trees, our experimental fires may have also reduced tree anchorage provided by surface roots, given that trees with fewer neighbours were more prone to death by uprooting (Supporting Information Figure S2) than by snapping during the windstorm (Supporting Information Table S1).

Our results indicate that the windstorm caused more structural impacts on *B3yr* plot than the *B1yr*. This differential vulnerability to windstorms between treatment plots is probably related to the intensity and severity of previous fires. Specifically, the *B3yr* plot accumulated more fuel loads between fires than the plot *B1yr*. Furthermore, the 2007 drought may have further increased fire intensity and severity by increasing air dryness and fuel loads. As a result, fires were more intense and severe in *B3yr*, particularly along the forest edge. Thus, there was a thinned forest canopy (only 143 trees/ha) in the *B3yr* plot compared to that of *B1yr* (234 trees/ha). The *B3yr* plot had more gaps, and more uprooted and snapped trees than *B1yr*. These results indicate that areas subjected to high-intensity fires have a higher vulnerability to wind damage. It is important to note that because most wildfires across the region occur in extremely dry years, the 2007 fire event was probably more representative than the experimental fires conducted during nondrought years (Brando et al., 2014).

4.2 | High mortality rates among large trees lead to substantial biomass losses

Although trees can become more mechanically stable as they grow (Ribeiro et al., 2016), we found that large trees were disproportionately affected by the windstorm, as previously reported (Canham, Papaik, & Latty, 2001; Rifai et al., 2016). In our experimental areas, the effects of previous fires on forest structure apparently intensified windstorm-related mortality of large trees. This pattern might be attributed to the fact that tall trees are more exposed to wind and

have larger crowns that together increase the strain on the root–soil interface and increase the likelihood of uprooting (Putz et al., 1983). Furthermore, although large trees can damage many other trees when they fall, only 20% of the damaged trees in our study were likely to be killed by other trees. These results have direct implications for forest carbon storage. In some regions of Amazonia and in other tropical forests, trees >50 cm DBH can store 50%–75% of the total above-ground forest biomass (Dewalt, Schnitzer, Denslow, Schniizert, & Julie, 2009; Fauset et al., 2015). Therefore, processes that preferentially kill large trees will have large impacts on forest carbon stocks. In our experimental area, the 30-min windstorm reduced above-ground forest biomass by 15%–31%. These reductions are comparable to the ones caused by low-intensity experimental fires conducted in the area between 2004 and 2010 (Brando et al., 2014).

4.3 | Trees with lower wood density are more vulnerable to wind damage

We found that trees with lower wood density are more likely to be uprooted or snapped than trees with high wood density. This finding supports the notion that wood density is one of the most important predictors of tree susceptibility to wind damage (Canham et al., 2010; Putz et al., 1983; Ribeiro et al., 2016; Rifai et al., 2016). Among the 19 most abundant genera in the study area, the one with the lowest average wood density (*Tapirira*) was damaged the most (Figure 1b). In contrast, four of the five least affected genera (*Chaetocarpus*, *Myrcia*, *Licania*, and *Mouriri*) have relatively high wood densities (>0.8 g/cm). An exception to this pattern was *Protium* (Burseraceae), which has wood of intermediate density (0.61 g/cm) but was among the five least damaged genera in our study site (Figure 1b). This genus was abundant only on the *Control* plot (89% of the total recorded *Protium* trees) and was represented mostly by small trees (10–15 cm DBH). Over the long term, as fires and fragmentation result in shifts in floristic composition towards communities with a high proportion of species with relatively lower wood densities (Laurance et al., 2006), forest vulnerability to windstorms will likely increase.

4.4 | Edge-exposed trees are more vulnerable to wind damage

Our results reinforce that observed increases in mortality of Amazonian trees in forest fragments (Laurance, Delamônica, Laurance, Vasconcelos, & Lovejoy, 2000) might be due to increased wind-related mortality near forest edges. As wind gusts become more intense and frequent on the edges of open fields (Bull & Reynolds, 1968; Mahmood et al., 2014; Weaver & Avissar, 2001), wind-caused tree mortality may contribute to observed replacement of slow-growing species with dense wood by species with opposing traits (Laurance et al., 2006). This process seems to be underway in our study area, where the average wood density of trees >20 cm DBH was lower near the forest edge (0.61 ± 0.13 g/cm^3) compared to the forest interior (0.64 ± 0.14 g/cm^3).

4.5 | Damaged trees die first in previously burned areas

The 2012 windstorm damaged proportionately more trees in the burned plots, and a larger proportion subsequently died in these plots than in the *Control* plot. These findings indicate that windstorms not only damage more trees in burned areas but also substantially increase greenhouse gas emissions even if some of the trees resprout (Marra et al., 2014; Putz & Brokaw, 1989). The observation that more of the wind-damaged trees in burned areas died 4 years after the windstorm also has relevant implications for forest flammability. This higher mortality creates more and larger canopy gaps, increases fuel loads, and can thereby increase the frequency and intensity of fires, thus leading to a positive feedback cycle.

5 | CONCLUSIONS

A windstorm damaged more trees and caused more biomass losses near the forest edge and in previously burned areas, which demonstrates the synergistic effects of natural and anthropogenic disturbances. We highlight that understorey fires can produce long-lasting effects on tropical forests not only by directly killing trees but also by increasing tree vulnerability to wind damage due to fire scars. At a regional scale, land-use and forest degradation are likely to increase forest vulnerability to wind disturbances, especially as ongoing climate changes are expected to increase the frequencies and intensities of windstorms.

ACKNOWLEDGEMENTS

This study was supported by a grant from the Brazilian Federal Government to S.E.T. in collaboration with the Department of Ecology of the University of Brasília (PVE – CNPq), by a postdoctoral fellowship to D.V.S. (PDJ – CNPq), and a financial support of PELD/CNPq (site TANG). The LiDAR dataset was acquired by the Sustainable Landscapes Brazil project supported by the Brazilian Agricultural Research Corporation (EMBRAPA), the US Forest Service, USAID, and the US Department of State.

AUTHORS' CONTRIBUTIONS

D.V.S. and P.M.B. designed the study, were involved in the data collection, and performed the statistical analyses. D.V.S., P.M.B., and F.E.P. wrote the paper. All authors discussed the results and commented on the manuscript.

DATA ACCESSIBILITY

Data available from the Dryad Digital Repository: https://doi.org/10.5061/dryad.3g14b02 (Silverio, 2018).

ORCID

Divino V. Silvério http://orcid.org/0000-0003-1642-9496
Paulo M. Brando https://orcid.org/0000-0001-8952-7025

REFERENCES

Araujo, R. F., Nelson, B. W., Celes, C. H. S., & Chambers, J. Q. (2017). Regional distribution of large blowdown patches across Amazonia in 2005 caused by a single convective squall line. *Geophysical Research Letters*, *44*(15), 7793–7798. https://doi.org/10.1002/2017GL073564

Asner, G. P., & Goldstein, G. (1997). Correlating stem biomechanical properties of Hawaiian canopy trees with hurricane wind damage. *Biotropica*, *29*(2), 145–150.

Attiwill, P. M. (1994). The disturbance of forest ecosystems: The ecological basis for conservative management. *Forest Ecology and Management*, *63*(2–3), 247–300. https://doi.org/10.1016/0378-1127(94)90114-7

Baker, P. J., Bunyavejchewin, S., & Robinson, A. P. (2008). The impacts of large-scale, low-intensity fires on the forests of continental Southeast Asia. *International Journal of Wildland Fire*, *17*(6), 782–792. https://doi.org/10.1071/WF07147

Balch, J. K., Nepstad, D. C., Brando, P., Curran, L. M., Portella, O., de Carvalho, O., & Lefebvre, P. (2008). Negative fire feedback in a transitional forest of southeastern Amazonia. *Global Change Biology*, *14*(10), 2276–2287. https://doi.org/10.1111/j.1365-2486.2008.01655.x

Barlow, J., Peres, C. A., Lagan, B. O., & Haugaasen, T. (2003). Large tree mortality and the decline of forest biomass following Amazonian wildfires. *Ecology Letters*, *6*(1), 6–8. https://doi.org/10.1046/j.1461-0248.2003.00394.x

Bivant, R., Altman, M., Anselin, L., Assunção, R., & Berke, O. (2016). *Spatial dependence: Weighting schemes, statistics and models*. Cran R Project. Retrieved from https://cran.r-project.org/web/packages/spdep/index.html

Brando, P. M., Balch, J. K., Nepstad, D. C., Morton, D. C., Putz, F. E., Coe, M. T., … Nobrega, C. (2014). Abrupt increases in Amazonian tree mortality due to drought-fire interactions. *Proceedings of the National Academy of Sciences of the United States of America*, *111*(17), 6347–6352. https://doi.org/10.1073/pnas.1305499111

Brando, P., Nepstad, D. C., Balch, J. K., Bolker, B., Christman, M. C., Coe, M. T., & Putz, F. E. (2012). Fire-induced tree mortality in a neotropical forest: The roles of bark traits, tree size, wood density, and fire behavior. *Global Change Biology*, *18*, 630–641. https://doi.org/10.1111/j.1365-2486.2011.02533.x

Broadbent, E., Asner, G., Keller, M., Knapp, D., Oliveira, P., & Silva, J. (2008). Forest fragmentation and edge effects from deforestation and selective logging in the Brazilian Amazon. *Biological Conservation*, *141*(7), 1745–1757. https://doi.org/10.1016/j.biocon.2008.04.024

Bull, G. A. D., & Reynolds, E. R. C. (1968). Wind turbulence generated by vegetation and its application. *Forestry Supplement*, *41*, 28–37.

Canham, C. D., Papaik, M. J., & Latty, E. F. (2001). Interspecific variation in susceptibility to windthrow as a function of tree size and storm severity for northern temperate tree species. *Canadian Journal of Forest Research*, *31*(1), 1–10. https://doi.org/10.1139/x00-124

Canham, C. D., Thompson, J., Zimmerman, J. K., & Uriarte, M. (2010). Variation in susceptibility to hurricane damage as a function of storm intensity in Puerto Rican tree species. *Biotropica*, *42*(1), 87–94. https://doi.org/10.1111/j.1744-7429.2009.00545.x

Chambers, J. Q. (2001). Tree damage, allometric relationships, and above-ground net primary production in central Amazon forest. *Forest Ecology and Management*, *152*(1–3), 73–84. https://doi.org/10.1016/S0378-1127(00)00591-0

Chambers, J. Q., Negron-Juarez, R. I., Marra, D. M., Di Vittorio, A., Tews, J., Roberts, D., … Higuchi, N. (2013). The steady-state mosaic of disturbance and succession across an old-growth Central Amazon forest landscape. *Proceedings of the National Academy of Sciences of the United States of America*, *110*(10), 3949–3954. https://doi.org/10.1073/pnas.1202894110

Chave, J., Andalo, C., Brown, S., Cairns, M. A., Chambers, J. Q., Eamus, D., … Yamakura, T. (2005). Tree allometry and improved estimation of carbon stocks and balance in tropical forests. *Oecologia*, *145*(1), 87–99. https://doi.org/10.1007/s00442-005-0100-x

Chave, J., Muller-Landau, H. C., Baker, T. R., Easdale, T. A., Steege, H., & Webb, C. O. (2006). Regional and phylogenetic variation of wood density across 2456 neotropical tree species. *Ecological Applications*, *16*(6), 2356–2367. https://doi.org/10.1890/1051-0761(2006)016[2356:RAPVOW]2.0.CO;2

Cliff, A. D., & Ord, J. K. (1981). *Spatial processes: Models and applications*. London, UK: Pion Ltd.

Cole, L. E. S., Bhagwat, S. A., & Willis, K. J. (2014). Recovery and resilience of tropical forests after disturbance. *Nature Communications*, *5*(May), 1–7.

Cook, B., Corp, L., Nelson, R., Middleton, E., Morton, D., McCorkel, J., … Montesano, P. (2013). NASA Goddard's LiDAR, Hyperspectral and Thermal (G-LiHT) Airborne Imager. *Remote Sensing*, *5*(8), 4045–4066. https://doi.org/10.3390/rs5084045

de Toledo, J. J., Magnusson, W. E., Castilho, C. V., & Nascimento, H. E. M. (2012). Tree mode of death in Central Amazonia: Effects of soil and topography on tree mortality associated with storm disturbances. *Forest Ecology and Management*, *263*, 253–261. https://doi.org/10.1016/j.foreco.2011.09.017

Dewalt, S. J., Schnitzer, S. A., Denslow, J. S., Schniizert, S. A., & Julie, S. (2009). Density and diversity of lianas along a chronosequence in a central Panamanian lowland forest. *Ecology*, *16*(1), 1–19.

Dray, S., Legendre, P., & Peres-Neto, P. R. (2006). Spatial modelling: A comprehensive framework for principal coordinate analysis of neighbour matrices (PCNM). *Ecological Modelling*, *196*(3–4), 483–493. https://doi.org/10.1016/j.ecolmodel.2006.02.015

Duffy, P. B., Brando, P., Asner, G. P., & Field, C. B. (2015). Projections of future meteorological drought and wet periods in the Amazon. *Proceedings of the National Academy of Sciences*, *112*(43), 201421010. https://doi.org/10.1073/pnas.1421010112

Durieux, L., Machado, L. A. T., & Laurent, H. (2003). The impact of deforestation on cloud cover over the Amazon arc of deforestation. *Remote Sensing of Environment*, *86*(1), 132–140. https://doi.org/10.1016/S0034-4257(03)00095-6

Emanuel, K. A. (2013). Downscaling CMIP5 climate models shows increased tropical cyclone activity over the 21st century. *Proceedings of the National Academy of Sciences*, *110*(30), 12219–12224. https://doi.org/10.1073/pnas.1301293110

Espírito-Santo, F. D. B., Gloor, M., Keller, M., Malhi, Y., Saatchi, S., Nelson, B., … Phillips, O. L. (2014). Size and frequency of natural forest disturbances and the Amazon forest carbon balance. *Nature Communications*, *5*, 3434. https://doi.org/10.1038/ncomms4434

Fauset, S., Johnson, M. O., Gloor, M., Baker, T. R., Monteagudo, M. A., Brienen, R. J. W., … Phillips, O. L. (2015). Hyperdominance in Amazonian forest carbon cycling. *Nature Communications*, *6*, 6857.

Fisher, R., McDowell, N., Purves, D., Moorcroft, P., Sitch, S., Cox, P., … Ian Woodward, F. (2010). Assessing uncertainties in a second-generation dynamic vegetation model caused by ecological scale limitations. *New Phytologist*, *187*(3), 666–681. https://doi.org/10.1111/j.1469-8137.2010.03340.x

Garstang, M., White, S., Shugart, H. H., & Halverson, J. (1998). Convective cloud downdrafts as the cause of large blowdowns in the Amazon rainforest. *Meteorology and Atmospheric Physics*, *67*(1–4), 199–212. https://doi.org/10.1007/BF01277510

Griffith, D. A., & Peres-Neto, P. R. (2006). Spatial modeling in ecology: The flexibility of eigenfunction spatial analyses. *Ecology*, *87*, 2603–2613. https://doi.org/10.1890/0012-9658(2006)87[2603:SMIETF]2.0.CO;2

Haddad, N. M., Brudvig, L. A., Clobert, J., Davies, K. F., Gonzalez, A., Holt, R. D., … Townshend, J. R. (2015). Habitat fragmentation and its lasting impact on Earth's ecosystems. *Science Advances*, *1*(2), 1–9. https://doi.org/10.1126/sciadv.1500052

Hansen, M. C., Potapov, P. V., Moore, R., Hancher, M., Turubanova, S. A., Tyukavina, A., … Townshend, J. R. G. (2013). High-resolution global maps of 21st-Century forest cover change. *Science*, *342*(6160), 850–853.

Holbrook, N. M., & Putz, F. E. (1989). Influence of neighbors on tree form: Effects of lateral shade and prevention of sway on the allometry of Liquidambar styraciflua (Sweet Gum). *American Journal of Botany*, *76*(12), 1740–1749. https://doi.org/10.1002/j.1537-2197.1989.tb15164.x

Huler, S. (2004). *Defining the wind: The Beaufort scale, and how a nineteenth-century admiral turned science into poetry*. New York, NY: Crown Publishers.

Hunter, M. O., Keller, M., Morton, D., Cook, B., Lefsky, M., Ducey, M., … Schietti, J. (2015). Structural dynamics of tropical moist forest gaps. *PloS One*, *10*(7), e0132144. https://doi.org/10.1371/journal.pone.0132144

Hurst, J. M., Allen, R. B., Coomes, D. A., & Duncan, R. P. (2011). Size-specific tree mortality varies with neighbourhood crowding and disturbance in a montane Nothofagus forest. *PloS One*, *6*(10), e26670. https://doi.org/10.1371/journal.pone.0026670

INPE. (2016). Projeto Prodes: Monitoramento da floresta Amazônica Brasileira por satélite.

Jiao-Jun, Z., Xiu-Fen, L., Yutaka, G., & Takeshi, M. (2004). Wind profiles in and over trees. *Journal of Forestry Research*, *15*(4), 305–312. https://doi.org/10.1007/BF02844959

Laurance, W. F., & Curran, T. J. (2008). Impacts of wind disturbance on fragmented tropical forests: A review and synthesis. *Austral Ecology*, *33*(4), 399–408. https://doi.org/10.1111/j.1442-9993.2008.01895.x

Laurance, W. F., Delamônica, P., Laurance, S. G., Vasconcelos, H. L., & Lovejoy, T. E. (2000). Conservation: Rainforest fragmentation kills big trees. *Nature*, *404*(6780), 836–836.

Laurance, W. F., Nascimento, H. E. M., Laurance, S. G., Andrade, A. C., Fearnside, P. M., Ribeiro, J. E. L., & Capretz, R. L. (2006). Rain forest fragmentation and the proliferation of successional trees. *Ecology*, *87*(2), 469–482. https://doi.org/10.1890/05-0064

Ledru, M. P. (2001). Late Holocene rainforest disturbance in French Guiana. *Review of Palaeobotany and Palynology*, *115*(3–4), 161–176. https://doi.org/10.1016/S0034-6667(01)00068-9.

Mahmood, R., Pielke, R. A., Hubbard, K. G., Niyogi, D., Dirmeyer, P. A., McAlpine, C., … Fall, S. (2014). Land cover changes and their biogeophysical effects on climate. *International Journal of Climatology*, *34*(4), 929–953. https://doi.org/10.1002/joc.3736

Marra, D. M., Chambers, J. Q., Higuchi, N., Trumbore, S. E., Ribeiro, G. H. P. M., dos Santos, J., … Wirth, C. (2014). Large-scale wind disturbances promote tree diversity in a Central Amazon forest. *PloS One*, *9*(8), e103711. https://doi.org/10.1371/journal.pone.0103711

Mayle, F. E., Power, M. J., Abbott, M. B., Absy, M. L., Aragão, L. E. O. C., Malhi, Y., … Athens, J. S. (2008). Impact of a drier Early-Mid-Holocene climate upon Amazonian forests. *Philosophical Transactions of the Royal Society of London. Series B, Biological Sciences*, *363*(1498), 1829–1838. https://doi.org/10.1098/rstb.2007.0019

McDowell, N., Allen, C. D., Anderson-Teixeira, K., Brando, P., Brienen, R., Chambers, J., … Xu, X. (2018). Drivers and mechanisms of tree mortality in moist tropical forests. *New Phytologist*, https://doi.org/10.1111/nph.15027.

Mitchard, E. T. A., Feldpausch, T. R., Brienen, R. J. W., Lopez-Gonzalez, G., Monteagudo, A., Baker, T. R., … Phillips, O. L. (2014). Markedly divergent estimates of Amazon forest carbon density from ground plots and satellites. *Global Ecology and Biogeography*, *23*(8), 935–946. https://doi.org/10.1111/geb.12168

Negrón-Juárez, R. I., Chambers, J. Q., Guimaraes, G., Zeng, H., Raupp, C. F. M., Marra, D. M., … Higuchi, N. (2010). Widespread Amazon forest tree mortality from a single cross-basin squall line event. *Geophysical Research Letters*, *37*(16), 1–5. https://doi.org/10.1029/2010GL043733

Nelson, B. W., Kapos, V., Adams, J. B., Oliveira, W. J., & Braun, O. P. G. (1994). Forest disturbance by large blowdowns in the Brazilian Amazon. *Ecology*, *75*(3), 853–858. https://doi.org/10.2307/1941742

Nepstad, D. C., Stickler, C. M., Soares-filho, B., Merry, F., & Nin, E. (2008). Interactions among Amazon land use, forests and climate: Prospects for a near-term forest tipping point. *Philosophical Transactions of the Royal Society of London. Series B, Biological Sciences*, *363*, 1737–1746.

Nogueira, E. M., Fearnside, P. M., Nelson, B. W., & França, M. B. (2007). Wood density in forests of Brazil's "arc of deforestation": Implications for biomass and flux of carbon from land-use change in Amazonia. *Forest Ecology and Management*, *248*, 119–135. https://doi.org/10.1016/j.foreco.2007.04.047

Powell, T. L., Galbraith, D. R., Christoffersen, B. O., Harper, A., Imbuzeiro, H. M. A., Rowland, L., … Moorcroft, P. R. (2013). Confronting model predictions of carbon fluxes with measurements of Amazon forests subjected to experimental drought. *New Phytologist*, *200*(2), 350–365. https://doi.org/10.1111/nph.12390

Putz, F. E., & Brokaw, N. V. L. (1989). Sprouting of broken trees on Barro Colorado Island, Panama*Ecology*, *70*(2), 508–512. https://doi.org/10.2307/1937555

Putz, F. E., Coley, P. D., Lu, K., Montalvo, A., & Aiello, A. (1983). Uprooting and snapping of trees: Structural determinants and ecological consequences. *Canadian Journal of Forest Research*, *13*, 1011–1020.

R Core Team. (2016). *R: A language and environment for statistical computing*. Vienna, Austria: R Foundation for Statistical Computing.

Ribeiro, G. H. P. M., Chambers, J. Q., Peterson, C. J., Trumbore, S. E., Magnabosco Marra, D., Wirth, C., … Higuchi, N. (2016). Mechanical vulnerability and resistance to snapping and uprooting for Central Amazon tree species. *Forest Ecology and Management*, *380*, 1–10. https://doi.org/10.1016/j.foreco.2016.08.039

Rifai, S. W., Urquiza Muñoz, J. D., Negrón-Juárez, R. I., Ramírez Arévalo, F. R., Tello-Espinoza, R., Vanderwel, M. C., … Bohlman, S. A. (2016). Landscape-scale consequences of differential tree mortality from catastrophic wind disturbance in the Amazon. *Ecological Applications*, *26*(7), 2225–2237. https://doi.org/10.1002/eap.1368

Schwartz, N. B., Uriarte, M., DeFries, R., Bedka, K. M., Fernandes, K., Gutiérrez-Vélez, V., & Pinedo-Vasquez, M. A. (2017). Fragmentation increases wind disturbance impacts on forest structure and carbon stocks in a western Amazonian landscape. *Ecological Applications*, *27*(6), 1901–1915. https://doi.org/10.1002/eap.1576

Silverio, D. V. (2018). Data from: Fire, fragmentation, and windstorms: A recipe for tropical forest degradation. *Dryad Digital Repository*, https://doi.org/10.5061/dryad.3g14b02.

Silverio, D. V., Brando, P. M., Balch, J. K., Putz, F. E., Nepstad, D. C., Oliveira-Santos, C., & Bustamante, M. M. C. (2013). Testing the Amazon savannization hypothesis: Fire effects on invasion of a neotropical forest by native cerrado and exotic pasture grasses. *Philosophical Transactions of the Royal Society of London. Series B: Biological Sciences*, *368*, 20120427.

Trumbore, S., Brando, P., & Hartmann, H. (2015). Forest health and global change. *Science*, *349*(6250), 814–818.

VanDerWal, J., Falconi, L., Januchowski, S., & Storlie, L. S. (2015). *Species Distribution Modelling Tools (SDMTools): Tools for processing data associated with species distribution modelling exercises*. Retrieved from cran.r-project.org

Vanderwel, M. C., Coomes, D. A., & Purves, D. W. (2013). Quantifying variation in forest disturbance, and its effects on aboveground biomass dynamics, across the eastern United States. *Global Change Biology*, *19*(5), 1504–1517. https://doi.org/10.1111/gcb.12152

Weaver, C. P., & Avissar, R. (2001). Atmospheric disturbances caused by human modification of the landscape. *Bulletin of the American Meteorological Society*, *82*(2), 269–281. https://doi.org/10.1175/1520-0477(2001)082aabbb0269:ADCBHMaaabb2.3.CO;2

Zar, J. H. (1999). *Biostatical analysis (4ª)*. Upper Saddle River, NJ: Prentice-Hall.

Zuur, A. F., Ieno, E. N., Walker, N. J., Saveliev, A. A., & Smith, G. M. (2009). *Mixed effects models and extensions in ecology with R*. New York, NY: Springer.

SUPPORTING INFORMATION

Additional supporting information may be found online in the Supporting Information section at the end of the article.

How to cite this article: Silvério DV, Brando PM, Bustamante MMC, et al. Fire, fragmentation, and windstorms: A recipe for tropical forest degradation. *J Ecol*. 2018;00:1–12. https://doi.org/10.1111/1365-2745.13076